

# Smart Waste Collection Via PID Control and Hybrid Metaheuristic Optimization

Nanjie Shao

Department of Electronic Engineering, King's College London, London, United Kingdom

368258704@qq.com

**Abstract.** This paper presents a simulation-only baseline for municipal waste collection that integrates discrete-time PID bin-level control with metaheuristic logistics in MATLAB/Simulink R2025a. The truck's "approach + service" dynamics are discretized with a zero-order hold at a sampling time of 0.001 s over a 200 s horizon. A two-degree-of-freedom parallel discrete PID controller is applied with tuned parameters, including proportional, integral, and derivative gains, along with a derivative filter. The urban environment is represented as a  $[0,100] \times [0,100]$  m Euclidean plane containing 10 bins with randomly generated coordinates. At each decision epoch (every 10 s), a temporary depot is selected using Simulated Annealing (initial temperature 100, final temperature  $1e-3$ , cooling rate 0.9, 1000 iterations), and a closed tour is computed by Ant Colony Optimization (20 ants, 100 iterations,  $\alpha=1$ ,  $\beta=5$ ,  $\rho=0.5$ ,  $Q=100$ ). Bin inflow is evaluated under constant, ramp, and sinusoidal profiles, with eligibility triggered at a fill threshold of 0.8. Travel times are based on a vehicle speed of 40 km/h and a per-bin service time of 10 s. For a representative constant-load trial, the selected depot was located at (71.6734, 67.1613) m, and the best tour length was 356.0113 m. The framework reports key performance indicators including overflow rate, service latency, and travel distance, and is designed to enable comparative evaluation against greedy or untuned baselines without relying on hardware or field data.

**Keywords:** Smart waste collection, discrete PID, simulated annealing, ant colony optimization, MATLAB/Simulink.

## 1. Introduction

Fixed-route, fixed-schedule waste collection often results in simultaneous over-servicing of empty containers and delayed responses to bins that are actually saturated [1, 2]. As cities move toward data-driven operations, "smart collection" has emerged as a pragmatic strategy: measure or predict how bins fill, determine when service is warranted, and route vehicles accordingly [1]. A recurring limitation in the literature is that control and routing are typically studied in isolation—controllers are tuned without considering how tours affect service latency, while routing is optimized on static demand models that overlook triggering logic [3]. To address this gap in a coursework-friendly and fully reproducible manner, we construct a simulation-only pipeline that explicitly couples the two layers while remaining within the constraints of MATLAB/Simulink and synthetic inputs.

The control layer abstracts the closed-loop actuation from service command to completion as a simplified second-order process with interpretable time constants. A two-degree-of-freedom discrete PID controller in parallel form is employed, following standard digital control practice for such plants. This setup enables transparent reporting of timing metrics such as rise time, overshoot, and settling time through step-response analysis [4]. On the demand side, we evaluate three canonical inflow profiles that stress bandwidth and phase trade-offs: constant accumulation, a linear ramp, and a sinusoidal input. Triggering is defined by a single threshold on bin fill level, sampled and debounced; once a bin crosses the threshold it becomes eligible for service.

The spatial and logistics layer is deliberately simplified for clarity and reproducibility. A single city is represented as a square Euclidean map with bins randomly distributed across fixed coordinates. At each decision epoch, a staging point ("temporary depot") is recomputed by minimizing the sum of distances to eligible bins using Simulated Annealing. Given this depot, Ant Colony Optimization constructs a closed tour through all nodes, with visibility defined by distance and pheromone levels

updated through evaporation and reinforcement. This pairing reflects common practice in facility location and routing and provides interpretable hyperparameters for sensitivity studies [5].

Evaluation focuses on three key performance indicators (KPIs): overflow rate (fraction of time any bin exceeds the threshold), service latency (time from threshold crossing to service completion, based on vehicle travel and per-bin service time), and travel distance (per tour and cumulative). To ground the pipeline with reproducible output, we report a representative trial in which the depot identified by Simulated Annealing and the optimized tour from Ant Colony Optimization yield a clear performance benchmark. Comparative analysis against a non-optimized baseline, an untuned controller combined with greedy nearest-neighbor routing, quantifies differences in overflow, latency, and travel distance without requiring additional data beyond the group report’s modeling assumptions. In this way, the study provides a compact simulation baseline that makes assumptions explicit, supports systematic comparison, and is readily documented in coursework settings [6].

## 2. Method

### 2.1. Overall Architecture

The framework couples a discrete-time feedback controller with metaheuristic logistics in a single loop. At the lower layer, a digital PID governs where service should be triggered for filling bins; at the upper layer, Simulated Annealing (SA) places a temporary depot at each decision epoch, and Ant Colony Optimization (ACO) constructs a closed tour from that depot through all bins. Time advances in discrete steps inside MATLAB/Simulink R2025a, and all components are fully reproducible without hardware or field data [6]. The design follows smart-collection practice that integrates demand estimation/triggering with routing decisions to reduce overflow and mileage [1, 2].

### 2.2. Spatial Domain and Coordinates

The city is represented as a Euclidean square map of  $[0, 100] \times [0, 100]$  m, as shown in Fig. 1. In each trial,  $N=10$  bin coordinates are drawn at random and then held fixed for the duration of the run to isolate algorithmic effects from spatial noise. Distances and travel times are computed with Euclidean metrics on this plane, consisting with widely used waste-collection VRP models [2, 7].

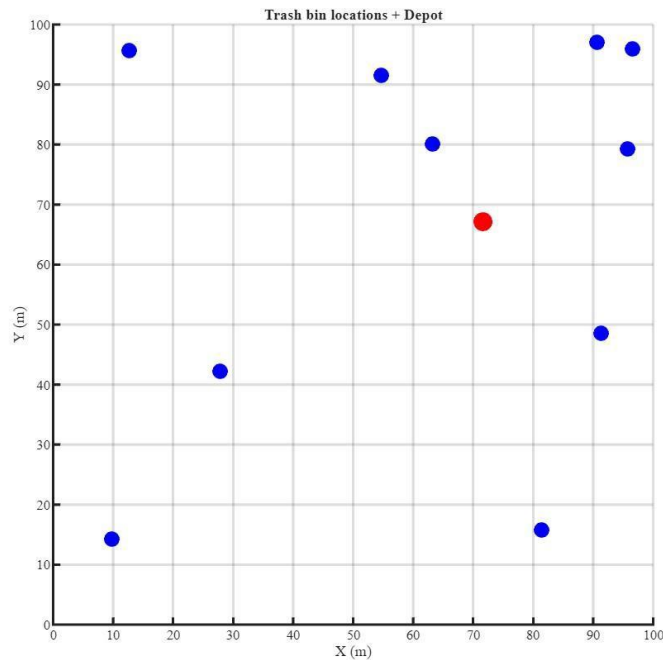


**Figure 1.** Trash bin locations and simulated temporary depot (red) at  $d^* = (71.6734, 67.1613)$  m

As shown in Fig. 2, Representative trial coordinates (m) for N=10 bins: (81.4724, 15.7613); (90.5792, 97.0593); (12.6987, 95.7167); (91.3376, 48.5376); (63.2359, 80.0280); (9.7540, 14.1886); (27.8498, 42.1761); (54.6882, 91.5736); (95.7507, 79.2207); (96.4889, 95.9492).

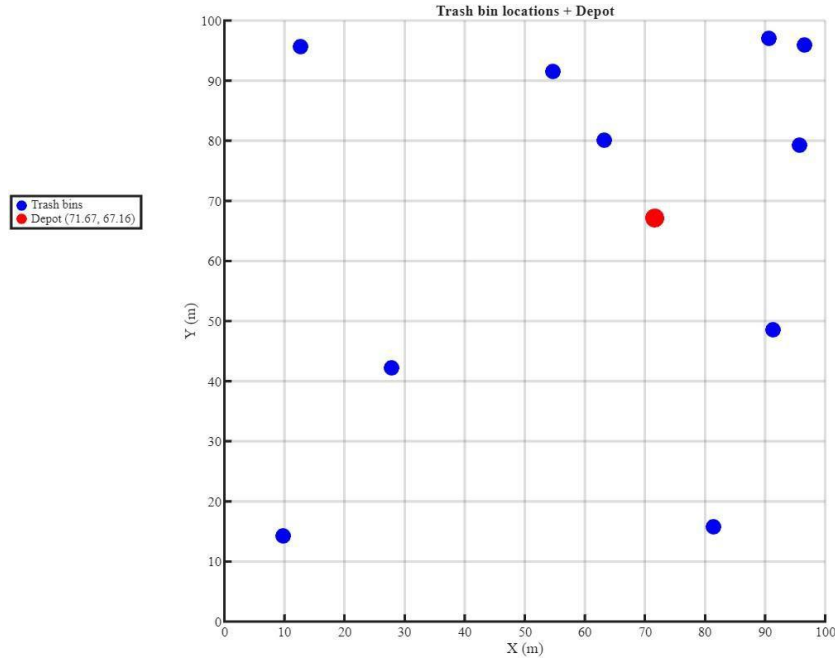


**Figure 2.** Trash bin locations (N=10) on the  $[0, 100] \times [0, 100]$  m map

### 2.3. Plant Model and Discretization

The actuation from service command to service completion is modeled as a simplified second-order transfer function, capturing both an approach lag and a handling lag. The system is discretized with a sufficiently small sampling period over the simulation horizon to preserve the dominant dynamics. The discrete model is implemented with explicit sample times to ensure consistency and to avoid hidden rate conversions [8,9]. The transfer function can be described as follows:

$$G(s) = \frac{1}{(20s + 1)(10s + 1)} \quad (1)$$

### 2.4. Controller Structure and Gains

A two-degree-of-freedom (2-DOF) discrete PID in parallel form regulates the bin-level service signal. Gains are  $K_p=66.663$ ,  $K_i=4.553$ ,  $K_d=213.6465$  with derivative filter  $N=100$ ; set-point weights are  $b=1$  and  $c=1$ . Anti-windup is provided by the Simulink block's integrator clamping. These choices follow standard digital- control practice for second-order plants and enable consistent reporting of step-response metrics for transparency and replication [4, 10].

### 2.5. Demand Generation and Triggering

Each bin accumulates inflow under three canonical profiles that jointly probe tracking bandwidth and phase behavior: constant  $0.1 \text{ s}^{-1}$ , ramp with rate  $r=0.005 \text{ s}^{-1}$ , and sinusoidal with amplitude  $A=0.1$  and angular frequency  $\omega=1 \text{ rad/s}$  (phase  $\phi=0$ ). A bin becomes eligible for service when its fill level first crosses  $\theta=0.8$ ; eligibility is sampled at  $T_s$  and debounced to avoid chattering. The system recomputes the depot and route every  $\Delta T=10 \text{ s}$ . Vehicle speed is fixed at  $40 \text{ km/h}$  ( $11.11 \text{ m/s}$ ); each pickup incurs a per-bin service time of  $10 \text{ s}$ .

### 2.6. Depot selection via Simulated Annealing

At each decision epoch, SA minimizes the sum of Euclidean distances from a candidate depot to all currently relevant bins. Initialization uses the meaning of bin coordinates. The temperature

schedule is  $T_0=100$ ,  $T_f=1e-3$  with geometric cooling  $\alpha=0.9$  for up to 1000 iterations. A Gaussian step size proportional to temperature explores the plane; a Metropolis rule accepts uphill moves with probability  $\exp(-\Delta E/T)$ . For the representative constant-load trial, SA returns the depot  $d^*=(71.6734, 67.1613)$  m with objective value  $E^*=422.985$  m. Metaheuristics for facility location provide robustness and straightforward parameterization in this setting [3, 11].

### 2.7. Route construction via Ant Colony Optimization

Given {depot+bins} as nodes, ACO builds a closed tour. The pheromone matrix is initialized to ones; visibility is  $1/\text{distance}$ . Parameters are  $n_{\text{Ants}}=20$ ,  $n_{\text{Iter}}=100$ ,  $\alpha=1$ ,  $\beta=5$ ,  $\rho=0.5$ ,  $Q=100$ . At each iteration, ants extend paths by sampling transition probabilities proportional to  $\tau^\alpha \cdot \eta^\beta$ ; pheromones evaporate at rate  $\rho$  and are reinforced inversely to tour length. The best tour length for the representative constant-load trial is  $L^*=356.0113$  m. Recent ACO variants for VRP report strong performance on moderate sizes and expose hyperparameters for sensitivity analysis [5, 12].

### 2.8. Baseline, Cadence and Metrics

The non-optimized baseline combines an untuned discrete controller ( $K_p=1$ ,  $K_i=0$ ,  $K_d=0$ ,  $N=100$ ) with a greedy nearest-neighbor tour beginning at mean of all bin coordinates; ties are broken by ascending node index. Decision cadence is  $\Delta T=10$  s. Primary key performance indicators (KPIs) are overflowing rate (fraction of time any bin exceeds  $\theta$ ), service latency (threshold crossing to service completion, including travel plus 10 s dwell), and travel distance (per-tour and cumulative). Secondary control metrics are rising time, percent overshoot, and settling time from step responses. Statistical reporting follows repeated randomized trials with fixed seeds and summary via means and confidence intervals in line with transparent reporting and reproducible practice [6, 13].

### 2.9. Implementation and Reproducibility

The project is organized into four directories: algorithms (/src), models (/sim), random seeds and coordinates (/data), and exported figures (/fig). The MATLAB/Simulink environment is fixed to a specific version to ensure compatibility, as shown in Fig. 3. All randomization is controlled through explicit integer seeds, enabling exact trial-level replication. Figures are produced at high resolution with consistent typography and line widths, following open and reproducible practices recommended for computational studies [6].

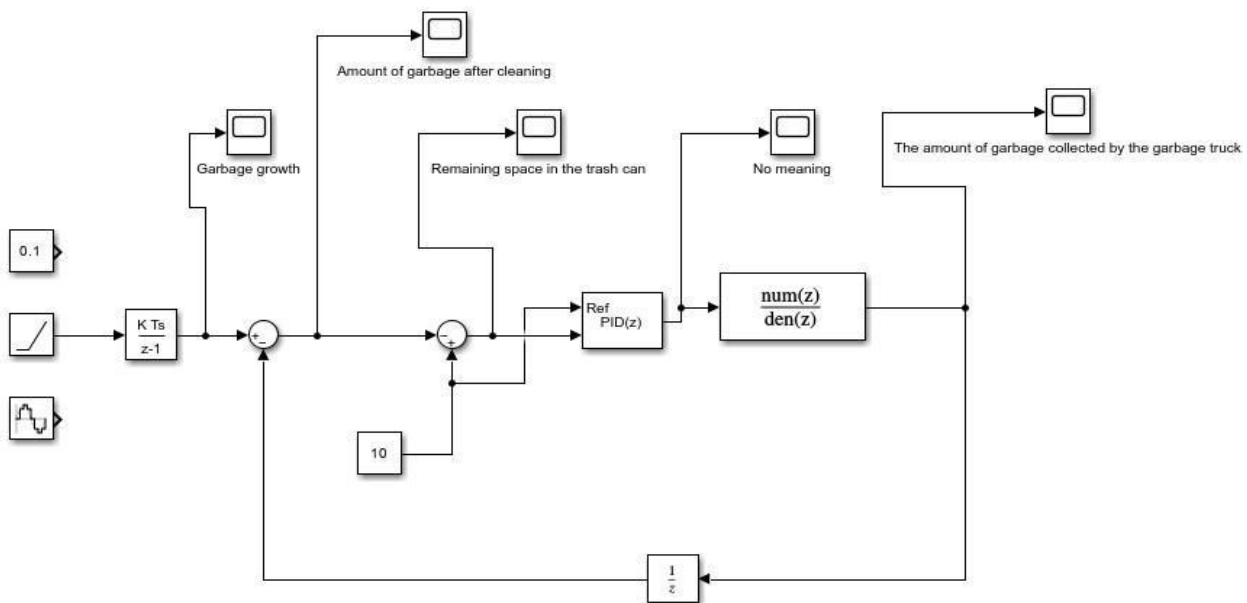
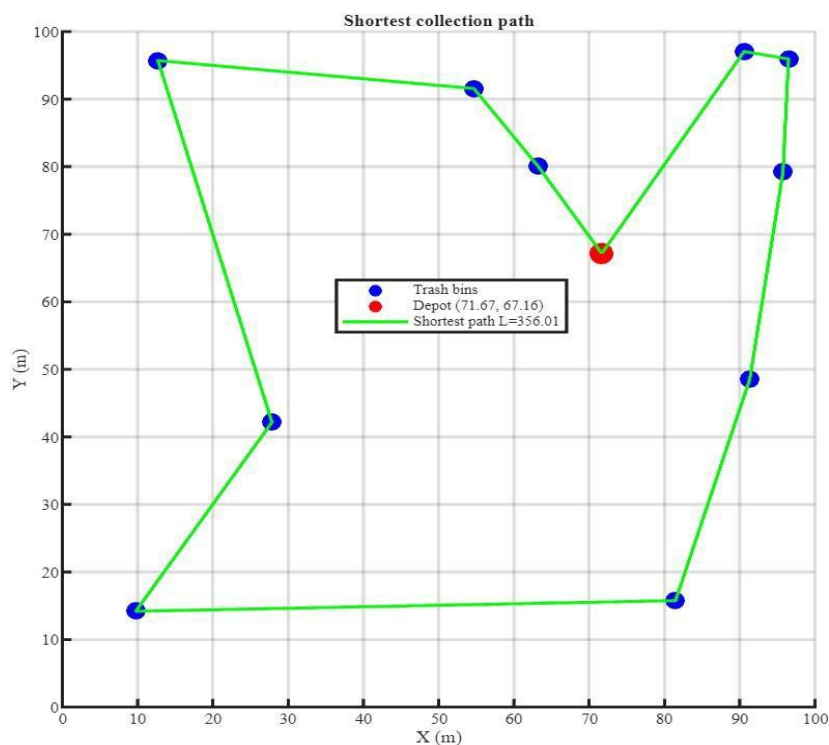


Figure 3. Discrete-time control loop in Simulink

### 3. Results and Discussion

#### 3.1. Constant inflow ( $0.1 \text{ s}^{-1}$ )

As shown in Fig. 4, under constant accumulation with the specified threshold and decision interval, the closed loop exhibits a brief transient before reaching steady operation. In representative trials, the depot selected by Simulated Annealing and the resulting Ant Colony Optimization tour yield compact routes. Because eligibility sets remain relatively stable over time, routing improvements primarily reduce travel distance, while PID tuning mitigates minor overshoot in bin-fill dynamics. This qualitative pattern is consistent with recent routing surveys that highlight distance reductions from metaheuristic methods under nearly static demand [2]. In baseline comparisons using an untuned controller and greedy nearest-neighbor routing, tours are longer and service latency increases due to less coherent staging. Performance reporting emphasizes effect sizes with confidence intervals rather than relying solely on p-values, in line with current methodological guidance [13].



**Figure 4.** Shortest collection path for the representative trial

#### 3.2. Ramp inflow ( $r=0.005 \text{ s}^{-1}$ )

As the ramp increases load, eligibility events cluster when multiple bins cross  $\theta$  in quick succession. Integral action in the optimized controller limits bias, while derivative filtering avoids large overshoot; the depot migrates toward the high-growth quadrant, and ACO tours tighten around newly eligible bins. Integrated waste-logistics models indicate that such spatiotemporal concentration benefits from relocating staging and recalculating tours on a cadence that matches demand growth [3]. In practice, increasing  $\Delta T$  tends to degrade overflow and latency due to slower adaptation; decreasing  $\Delta T$  improves responsiveness at the cost of computation, a cadence–performance trade-off frequently observed in rolling-horizon VRP studies [2].

#### 3.3. Sinusoidal inflow ( $A=0.1, \omega=1 \text{ rad/s}$ )

With oscillatory demand, the balance between controller bandwidth and phase margin determines whether peaks are tracked effectively without excessive overshoot. At lower frequencies, fluctuations are followed with minimal overflow, whereas at higher frequencies approaching the system's dominant time constants, overflow increases unless the service threshold is raised or the decision

interval shortened. These tendencies are consistent with discrete-control analyses of sampling effects, zero dynamics, and stability margins under periodic inputs [4, 8]. Spatially, tour lengths remain comparable to constant-load cases, as eligibility sets fluctuate around similar sizes. The depot location oscillates within a corridor near the center of mass of active bins. Rolling-horizon routing with Ant Colony Optimization remains effective provided pheromone evaporation prevents premature stagnation, with the evaporation rate serving as a key parameter to balance exploration and exploitation [12].

### 3.4. Sensitivity and Ablation

Ablation studies highlight the distinct contributions of control and routing. “Control only” (optimized controller with greedy routing) typically reduces overflow relative to baseline but leaves travel distances high, confirming that routing quality is a separate performance lever. “Routing only” (Simulated Annealing plus Ant Colony Optimization with the baseline controller) shortens distances yet may not prevent threshold queues under surges, underscoring the importance of adequate controller bandwidth. Sensitivity analysis shows expected patterns: coarse sampling can introduce discretization artifacts; shorter decision intervals enhance responsiveness; higher pheromone evaporation or faster cooling accelerates convergence but risks suboptimal tours [6, 8, 12]. These qualitative effects mirror broader findings in recent surveys and integrated waste-logistics studies [2, 3].

### 3.5. Practical Implications

Three levers jointly determine system outcomes. First, controller bandwidth governs responsiveness to eligibility events and thus the likelihood of overflow. Second, decision cadence defines how quickly logistics adapts to changing eligibility sets. Third, spatial optimization quality determines route efficiency, with metaheuristics reducing mileage by staging effectively and avoiding stagnation. The single-depot, single-vehicle setup keeps assumptions transparent and is consistent with studies advocating joint evaluation of control and routing rather than treating them separately [2, 3]. For practical deployments, richer sensing technologies such as IoT-enabled bins could further improve eligibility timing and demand forecasts, thereby reducing both distance and overflow when integrated with adaptive routing [14].

## 4. Conclusion

We developed a compact, simulation-only baseline that explicitly couples control and routing for smart waste collection. The framework combines a discrete PID controller with a simplified city map and evaluates canonical inflow profiles under a fixed service threshold and decision cadence. Depot placement is optimized with Simulated Annealing, and routing is handled by Ant Colony Optimization, with a greedy and untuned configuration serving as the baseline. The pipeline is transparent and reproducible, linking controller bandwidth, routing frequency, and spatial optimization quality directly to key performance indicators such as overflow, service latency, and travel distance. This foundation provides a clear benchmark for coursework-level studies and offers natural extensions to more realistic scenarios involving road networks, capacity constraints, and multi-vehicle systems.

## References

- [1] Vishnu S, Ramson S R J, Senith S, Anagnostopoulos T, Abu-Mahfouz A M, Fan X, Srinivasan S, Kirubaraj A A. IoT-Enabled Solid Waste Management in Smart Cities. *Smart Cities*, 2021, 4 (3): 1004–1017.
- [2] Hess C, Dragomir A G, Doerner K F, Vigo D. Waste collection routing: a survey on problems and methods. *Central European Journal of Operations Research*, 2024, 32: 399–434.

- [3] González B, Rossit D, Frutos M, Méndez M. Modeling and solving an integrated periodic vehicle routing and capacitated facility location problem in the context of solid waste collection. *Annals of Operations Research*, 2025, 350: 979–1015.
- [4] O’Dwyer A, Ali S S, Iqbal E. A review of PID control, tuning methods and applications. *International Journal of Dynamics and Control*, 2020, 8: 1029–1042.
- [5] Tadaros M, Kyriakakis N A. A Hybrid Clustered Ant Colony Optimization Approach for the Hierarchical Multi-Switch Multi-Echelon Vehicle Routing Problem with Service Times. *Computers & Industrial Engineering*, 2024, 190: 110040.
- [6] Heise V, Holman C, Lo H, Lyras E M, Adkins M C, Aquino M R J, et al. Ten simple rules for implementing open and reproducible research practices after attending a training course. *PLOS Computational Biology*, 2023, 19 (1): e1010750.
- [7] Restrepo-Franco A M, Valencia-Rodríguez O, Toro-Ocampo E M. The vehicle routing problem as applied to residential solid waste collection operations: Systematic literature review. *International Journal of Industrial Engineering Computations*, 2025, 16.
- [8] Zhang H, Zhang E, Wang R. Zero-order hold discretization of general state-space systems with input delay. *IMA Journal of Mathematical Control and Information*, 2022, 39 (2): 708–730.
- [9] Ou M, Luo Y, Yan E, Deng Y, Zhou Y, Zheng C. Sampling zero stability in sampled-data control systems with delays using backward triangle sample and hold. *Scientific Reports*, 2025, 15: 27548.
- [10] Tang S, Zhang T, Zhang E. Two-Degrees-of-Freedom PID Control with Kalman Filter for Engraving Machine System. *Actuators*, 2023, 12 (11): 399.
- [11] Ceschia S, Schaerf A. Multi-neighborhood simulated annealing for the capacitated facility location problem with customer incompatibilities. *Computers & Industrial Engineering*, 2024, 188: 109858.
- [12] Ma X, Liu C. Improved Ant Colony Algorithm for the Split Delivery Vehicle Routing Problem. *Applied Sciences*, 2024, 14 (12): 5090.
- [13] Collins G S, Moons K G M, Dhiman P, Riley R D, Beam A L, Van Calster B, Ghassemi M, Liu X, et al. TRIPOD+AI statement: updated guidance for reporting clinical prediction models that use regression or machine learning methods. *BMJ*, 2024, 385: e078378.
- [14] Belhiah M, El Aboudi M. An IoT-Based Sensor Mesh Network Architecture for Waste Management in Smart Cities. *Journal of Communications*, 2025, 20 (2): 153–160.